

REGULAR ARTICLE

A theoretical research on the impact of pyridine based and fused cyclic based polymer on the properties of donor polymer for organic solar cells

Yalin Ran, Xian Peng, Xiaoqin Tang, Xiaorui Liu, Wei Shen, Rongxing He, Ming Li*

Key Laboratory of Luminescence and Real-Time Analytical Chemistry (Southwest University), Ministry of Education, College of Chemistry and Chemical Engineering, Southwest University, Chongqing 400715, China.

Received 15 Nov. 2017; Accepted (in revised version) 25 Dec. 2017

Abstract: The polymer with D-A structure has been certified a significant role as donor materials of organic solar cells (OSCs) for its outstanding light absorption. In this work, the properties of pyridine based and fused cyclic based D-A polymer was studied by means of DFT and TD-DFT theory under PBE0/6-31G(d) level. Based on the reported polymer D1, pyridine and fused cyclic were introduced to D2, D3 and D4. Compared with polymer lacking the pyridine and fused cyclic, the pyridine and fused cyclic based exhibits better planarity, lower HOMO energy and broader absorption properties, which are helpful to get a higher V_{oc} and J_{sc} . Moreover, fused cyclic based as well as pyridine monocycle and pyridine fused cyclic based polymer shows the ability to enhance the hole transfer rate. Hence, the approach of introducing pyridine and fused cyclics to polymer donor is a feasible way to modulate the electron-withdrawing capability in D-A polymer chain thereby promotes the performance of the OPV devices.

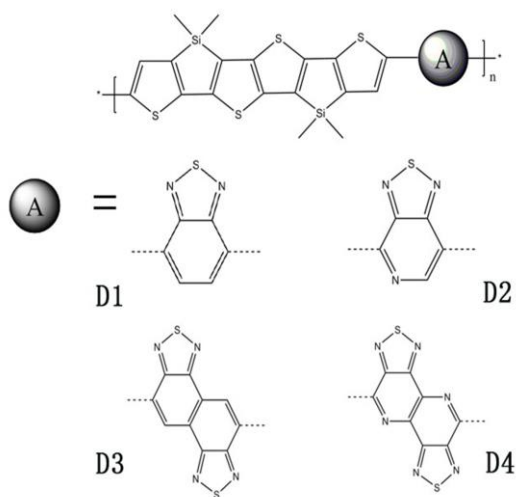
Keywords: Organic solar cells, density functional theory, D-A polymer, DFT, TD-DFT, absorption

* Corresponding author. *E-mail address:* liming@swu.edu.cn(Ming Li)
<http://www.global-sci.org/cicc>

1. Introduction

Polymer solar cells (PSCs) possess desirable characteristic such as low cost, flexibility and lightweight attracting much attention from academia [1]. In bulk-heterojunction solar cells (BHJSCs), the phase-separated donor/acceptor blend layer is constituted of conjugated polymers, and fullerene derivatives like [6,6]-phenyl-C61-butyric acid methyl ester (PC61BM) or [6,6]-phenyl-C71-butyric acid methyl ester (PC71BM) traditionally [2]. The D-A conjugated copolymers donor material in typical BHJSCs always comprises of electron rich moieties (donor, D) and electron deficient moieties (acceptor, A) [3]. A remarkable amount of effort in the past decades have made to improves the power conversion efficiency of BHJSCs largely. The state-of-the-art PCE of single-junction BHJSCs has been exceeded 10% and their tandem counterparts can achieve more in many research groups report recently. Such as jing bozhao et al. achieved a PCE of 11.7% by polymer donor material PffBT4T-C9H13 successfully.

In OPV devices, the open circuit voltage (V_{oc}), short-circuit current density (J_{sc}) and the fill factor (FF) are related to the power conversion efficiency (PCE). V_{oc} is related to the difference between the highest occupied molecular orbital (HOMO) energy level of donor materials and the lowest unoccupied molecular orbital (LUMO) energy level of acceptor materials. J_{sc} are mainly affected by the efficiency of light absorption, exciton diffusion, charge transfer and charge collection [4]. Hence, for conjugated donor copolymer materials, the high hole transfer rate with a deep HOMO level and good absorption properties is our present struggling object.



Scheme 1. The chemical structure of D1, D2, D3 and D4

Recently, Raja Shahid Ashraf and co-workers designed and synthesized Thieno[3,2-b]thienobis(silolothiophene) based D-A polymer donor. The polymer characters low band gap and appropriate spectrum matching the solar spectrum very well. Besides, the introduction of silicon among the adjacent aromatic units in electron rich moieties can lower the HOMO energy level, enlarge the conjugation length and diminish the conformations disorder.

However, it is clear that the electron deficient-moieties are equally important to the properties of D-A conjugated polymers. Benzothiadiazole (BT) is a widely used electron withdrawing group for its strong ability of accepting electron [5]. Compared with BT, thiadiazolo[3,4-c]pyridine (PT) is a stronger electron recipient due to the introduction of a more electron-deficient pyridine, which is less explored in D-A copolymers. In addition, pyridine based compounds could result in a higher electron affinity in the backbone and leads to narrower optical gaps. Shu Seki et al and Alan J. Heeger et al. reported the performance of enhancement impact of PT as the electron withdrawing group. Hence PT was adopted in our work to investigate the effect of presence or absence of the pyridine unit to the D-A polymer.

Meanwhile, a fused cyclic compound naphtho[1,2-c:5,6-c']bis[1,2,5]thiadiazole (NT) was reported to improve short-circuit current (J_{sc}) and photovoltaic performance as an electron withdrawing group. In 2012, Jinwei Gao et al use NT units promoted the performance of the devices. The unit of fused ring, NT, also gets a stronger electron withdrawing capability than BT, which are potential to enhance the performance of the polymer. Although the pyridine and fused cyclic compound based polymer achieved preferable effect, their relations to molecular structure, energy level, and hole transfer properties still need to be further explored. Meanwhile, The coexist interaction effect of pyridine and fused cyclic compound

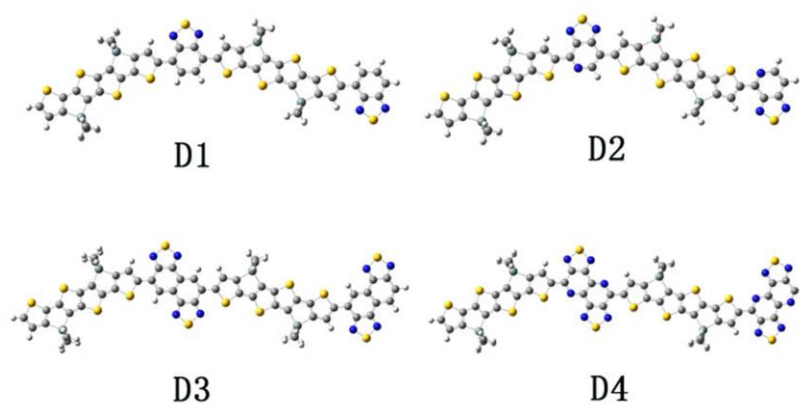


Figure 1: The configurations of 4 optimized dimers

remains to be seen. And how the molecular structure affect electron withdrawing intensity and thus the performance of PSCs deserved to be explored theoretically. To understand these relationships, on the basis of synthesized donor copolymer (D1) linking benzothiadiazole(BT) as acceptor unit, thiadiazolo [3,4-c]pyridine (PT) based dimer (D2), fused cyclic benzothiadiazole (2BT) based (D3) and fused cyclic pyridine (2PT) (D4) (shown in **Scheme 1**) were designed and researched. The calculated HOMO energy levels and the band gaps are used quantum-chemical method. Besides, the hole transfer properties of these dimers were investigated for further estimating of the performance.

2. Computational methods

For the present work, the ground state geometry structure of copolymers (dimer models) were optimized by adopting density functional theory (DFT) [6] under B3LYP [7], PBE0 [8], BHandHLYP [9], B3P86 [10] functional at 6-31G(d) basis set levels. Compared with experimental data, PBE0 method achieved a more accurate HOMO level. In this work, all the side chain alkyl of dimers was replaced by methyl, because the side chain alkyl merely improves the solubility without alter the electronic properties [11, 12]. Based on optimized structure of dimers under PBE0/6-31G(d) level, the electronic absorption properties were investigated via time-dependent density functional theory(TD-DFT) under PBE0, PW91PW91 , B3LYP, BHandHLYP, BMK , M06 [14], M05 , and functional at 6-31G(d) basis set levels. Compared with experimental data, M05 method attained more precise absorption properties. Besides, Multiwfn 2.1 software was applied to visualize the electron densities of all orbital that related to electronic transitions. Finally is the caculation of the carrier drift mobilities and its related parameter. As for reorganization energy, the neutral and cation geometry structures were carried out under PBE0/6-31G(d) level. And face to face molecular stacking is manually assembled by gaussview software. MPW1PBE, MPW1LYP, PW91, M062X, PBE0 and B3PW91 functional under 6-31G(d) basis level were chosen to find the most stable position of two adjacent segments. Scanning plots result shows that M062X can find the most stable π -stacking distance of two adjacent segments. On the basis of the stable structure of the two adjacent segments, ADF software is used to calculate the hole coupling

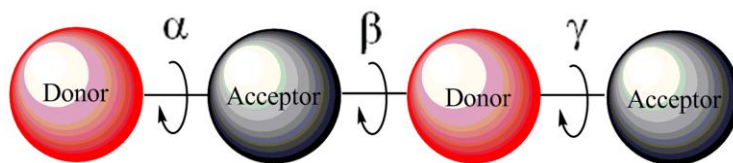


Figure 2: The link order of studied dimer

strength. In this work, all DFT and TD-DFT calculations were achieved by Gaussian 09 software packages [15].

3. Results and discussions

3.1 Configurations

The configuration of the copolymer has a close relation with the properties of the material [16]. The optimized structures of four dimers were exhibited in **Figure 1**. According to the link order of Donor-Acceptor-Donor-Acceptor (**Figure 2**), the dihedral angle between the donor section and acceptor section of four dimers was compared, and results were shown in **Table 1**.

Table 1. The dihedral angle of studied dimer

	α (D-A)	β (A-D)	γ (D-A)
D1	175.99°	175.66°	179.98°
D2	179.89°	178.36°	179.99°
D3	175.58°	172.45°	179.06°
D4	179.99°	179.99°	180.00°

In the results, the dihedral angle α , β and γ of pyridine based D2 and D4 are larger than D1 and D3 due to the reduction of steric hindrance by the replacement of C to N atom. The planarity D3 and D4 are superior to D1 and D2 because of the interplay of intramolecular noncovalent coulomb interactions between the N atom in fused cyclic and sulfur atom beside the fused cyclic [17].

3.2 Frontier molecular orbital and photovoltaic properties

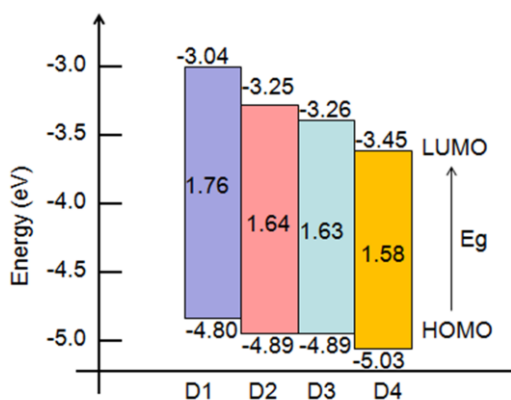


Figure 3: The energy of HOMO/LUMO and the E_g values of 4 dimers

The frontier molecular orbital of copolymers are related to open-circuit voltage (V_{oc}) and the energy gap of organic solar cells [18, 19]. The value of V_{oc} is based on the highest occupied molecular orbital (HOMO) of donor materials and the lowest unoccupied molecular orbital (LUMO) of acceptors materies according to the equation (1) [20, 21].

$$V_{oc} = (1/e)(|E^D HOMO| - |E^A LUMO|) - 0.3V \quad (1)$$

A lower HOMO can generate a higher V_{oc} which is needed for good donor material. The energy gap (Eg) is the energy difference of HOMO and LUMO which has a crucial influence on optical behavior [22, 23]. A narrow Eg can improve the absorption behavior thus increase the J_{sc} . Hence the calculation and comparison of the HOMO levels and Eg for the investigated polymer donors are necessary.

In this work, we have used four functions to calculate HOMO values and ten function to calculate Eg value on the 6-31G(d) basis level for D1. Comparing with the experimental data (see in supporting information Table S1 and Table S2), the calculated results of HOMO (-4.80 eV) under PBE0/6-31G(d) level and Eg 1.76 eV (704 nm) under m05/6-31G(d) level are more closely to the experimental value (HOMO:-5.00 eV, λ_{max} : 694 nm) [24]. Hence, we adopt the functional above to investigate the HOMO and Eg values of 4 dimers. For the inaccuracy of theoretical calculation of LUMO, we take the equation (2) to calculate LUMO [25, 26]. The calculated results of 4 dimers were shown in **Figure 3**.

$$E_{LUMO} = E_{HOMO} + E_g \quad (2)$$

HOMO levels of pyridine based D2 and D4 (-4.89 and -5.03 eV) are lower than D1 and D3 (-4.80 and -4.89 eV), besides the HOMO of fused cyclic based D3 and D4 (-4.89 and -5.03 eV) are lower than D1 and D2 (-4.80 and -4.89 eV). In addition, Eg levels of pyridine based and fused cyclic based dimers show the identical superiority compared with their

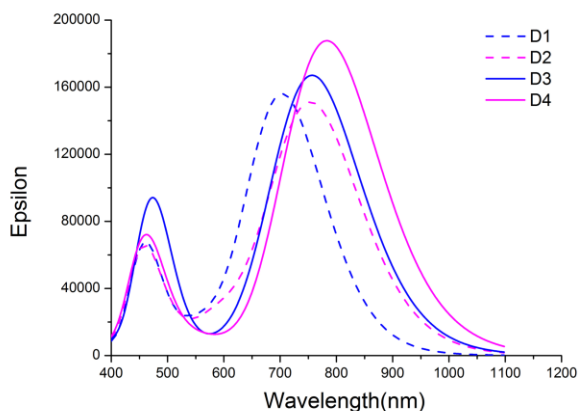
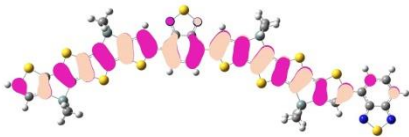
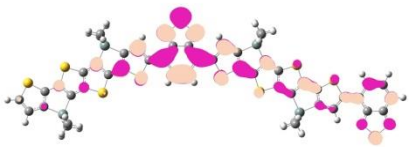
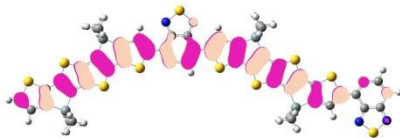
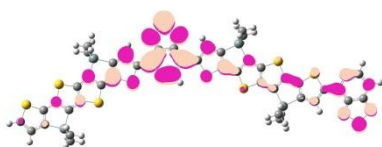
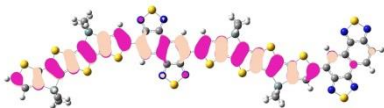
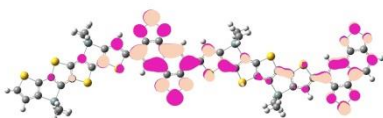
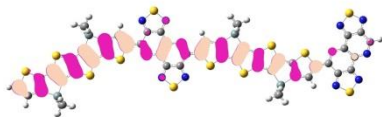



Figure 4: Simulated absorption spectra of studies dimers

counterpart. That means the pyridine based and fused cyclic based donor polymer can enhance the V_{oc} and optical behavior for organic solar cells.

Meanwhile, we draw the frontier molecular orbital of the four dimers on **Table 2**. Put insight on these plots we will find all the plots is shown strong π conjugated effect. And the HOMO is distributed on the whole molecular backbone, while the LUMO are mainly concentrated on electronic deficient unit. Electronic transfer of intramolecular is from the HOMO to LUMO.

Table 2. Electron density plots of HOMO and LUMO

Dimers	HOMO	LUMO
D1		
D2		
D3		
D4		

3.3 Absorption spectra

The donor section is a key unit to absorb sunlight in photovoltaic devices. As for the polymer donor, a broad and intensive absorption property is needed. Besides, a matching absorption range of the combined polymer donor and fullerene acceptor with solar UV-visible spectrum affects the efficiency of the device as well. We adopt one ideal model which makes polymer donor parallel with fullerene acceptor to simulate the absorption of combined polymer donor and fullerene acceptor. **Figure 4** and **Figure 5** provide the simulated absorption spectra of four individual donor dimers and combined donor-PC61BM. Related informations of absorption are given on **Table 3** and **Table 4**.

As show in **Figure 4** and **Figure 5**, the absorption ranges of these four dimers cover the solar spectrum (300-800nm) very well. When combined with PC61BM, the absorption band was broaden from 600-1100nm to 400-1400nm, thus a better matching of absorption with the solar spectrum in visible and near-infrared range is obtained.

As shown in **Table 3**, compared with D1 and D3 (704.29 and 758.76 nm), the maximum absorption wavelength of pyridine based D2 and D4 (755.80 and 784.06 nm) exhibits a trend of red-shift, and fused cyclic based D3 and D4 (758.76 and 784.06 nm) shows the same trend when contrasted with D1 and D2 (704.29 and 755.80 nm). This trend is consistent with the decreasing of the energy gap (the sequence of the four dimers is $1.76 > 1.64 > 1.63 > 1.58\text{eV}$). That is to say the unit consist of pyridine has better absorption effect than benzothiadiazole. Meanwhile, fused cyclic based benzothiadiazole and pyridine all show better absorption properties comparing to monocycle based polymer. The main transitions of S1 state for all

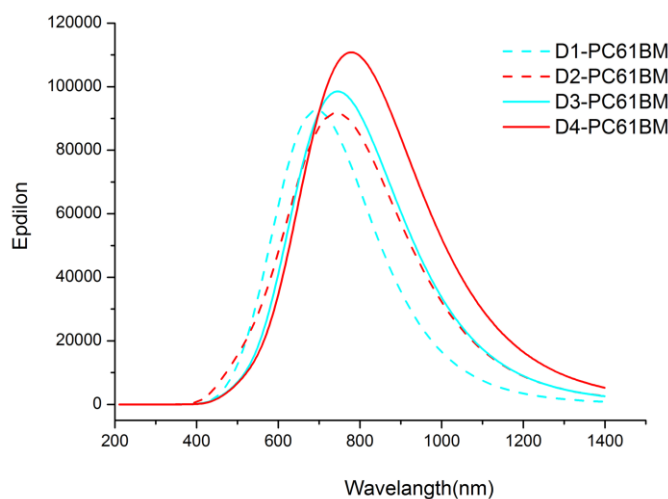


Figure 5: Simulated absorption spectra of combined donor-PC61BM dimers

dimers are corresponding to the transition from HOMO to LUMO, and the second absorption band of these dimers contains the translation of several orbits. All the translation is intramolecular translation of $\pi \rightarrow \pi^*$.

The electron density difference plots of four individual donor dimers and combined PC61BM acceptor were illustrated in **Figure 6** for an in-depth research of the exciton dissociation. We have drawn translation of $S_0 \rightarrow S_1$ state. Some data have been collected in **Figure 6**. D is the electron transfer distance. O is the overlap of the increasing or decreasing of the electron density and Δq is the fraction of exchanged electron. In this plot, the light green and the purple area are corresponding to the electron-rich donor moieties and electron-deficiency acceptor moieties respectively. In other words, the light green and purple elucidates the decrease with the increase of electron densities respectively. As shown in the plot, electron transfer is from the light green area to the purple area. Transitions of $S_0 \rightarrow S_1$ state are mainly from the trailing electron-rich moieties to central electron-deficiency moieties. The results in **Figure 4** revealed that both the hole transfer distance and the fraction of exchanged electron are improved in such designed scheme especially in fused cyclic based polymers. The D and Δq of D4 are 14.49 and 1.03 which is obviously increased. It shows that the pyridine and fused cyclic based polymers have a better intramolecular charge transfer that resulting in a much broader absorption spectra in the visible and infrared region.

3.4 Hole transfer properties

According to the working mechanism of an organic solar cell, the last step is the transfer and collection of free charge on the respective electrode. In our research, we used to focus hole transfer on donor material and electron to acceptor material. A High hole transfer rate for the polymer donors can enhance the charge transport efficiency in polymer organic solar cells. [27] Commonly we take hopping model to describe carrier transport in materials at room temperature. According to this theoretical model Einstein equation can be used to calculate carrier drift mobility.

$$\mu = \frac{eD}{k_B T} \quad (3)$$

where k_B , T , e , D represent the Boltzmann constant, the temperature (298.15 K), electronic charge, charge diffusion constant respectively. In spatially isotropic system, D can be defined by equation (4).

$$D = \lim_{t \rightarrow \infty} \frac{1}{2d} \frac{\langle x(t)^2 \rangle}{t} \approx \frac{1}{2d} \sum_i r_i^2 K_i P_i \quad (4)$$

d is the spatial dimension and i represents a specific hopping pathway. r_i , K_i represent π -stacking distance, charge transfer rate. $P_i = K_i / \Sigma$ and K_i is the electron hopping probability of the neighbor units. When only considering two adjacent molecular fragments.

D can be simply defined in (5).

$$D = \frac{1}{2} k_h r^2 \quad (5)$$

k_h is the hole transfer rate and r is the π - π stacking distance of nearest- neighbor pairs. Taking D into The Einstein equation can get the hole mobility (μ) expression.

$$\mu = \frac{e r^2}{2 K_B T} k_h \quad (6)$$

hole transfer rate k_h can be obtained from the classical Marcus theory: According to Marcus theory, the charge transfer rate is estimated by the equation (7) [28, 29].

$$k_h = \frac{v^2}{\hbar} \sqrt{\frac{\pi}{\lambda_h k_B T}} \exp\left(\frac{-\lambda_h}{4 K_B T}\right) \quad (7)$$

Where v , λ , are strength of coupling and reorganization energy, \hbar related to the Planck constant. K_B is the Boltzmann's constant, and T is defined as 300K. Hence, strength of coupling and reorganization energy is two crucial parameters need to know.

Generally, reorganization energy is divided into two parts: inner reorganization energy and outer reorganization energy, where the latter depends on the polarization of the medium around [30-32]. The theoretical and experimental research on charge transfer shows that the outer reorganization energy could be neglected in crystalline or amorphous states and inner reorganization could be calculated by using four point model methods [33]. According to this model, the energy of the neutral segment and the cation segment under the geometry of the neutral and the cation state respectively were calculated. The inner reorganization energy could be expressed as follows:

$$\lambda_i = [E^0(M^+) - E^0(M_0)] + [E^+(M_0) - E^+(M^+)] \quad (8)$$

Where $E^0(M_0)$ and $E^+(M_0)$ represent the energy of the neutral and the cation segment under the geometry of the neutral state respectively, $E^0(M^+)$ and $E^+(M^+)$ represent the energy of the neutral segment and the cation segment under the geometry of the cation state respectively [34].

Hole coupling strength (V_h), another key parameter, is generally calculated by ADF software on the base of optimized ground geometry statement by the Marcus-Hush model [31, 35-37]. The coupling strength can be expressed as follows [38, 39]:

$$V = \frac{J - S(\varepsilon_1 + \varepsilon_2)/2}{1 - S^2} \quad (9)$$

where J is the charge transfer integral, S is the overlap integral, ε is the grand state energy of per site. The electronic coupling strength is the charge transfer integral of the amended grand state energy of per site.

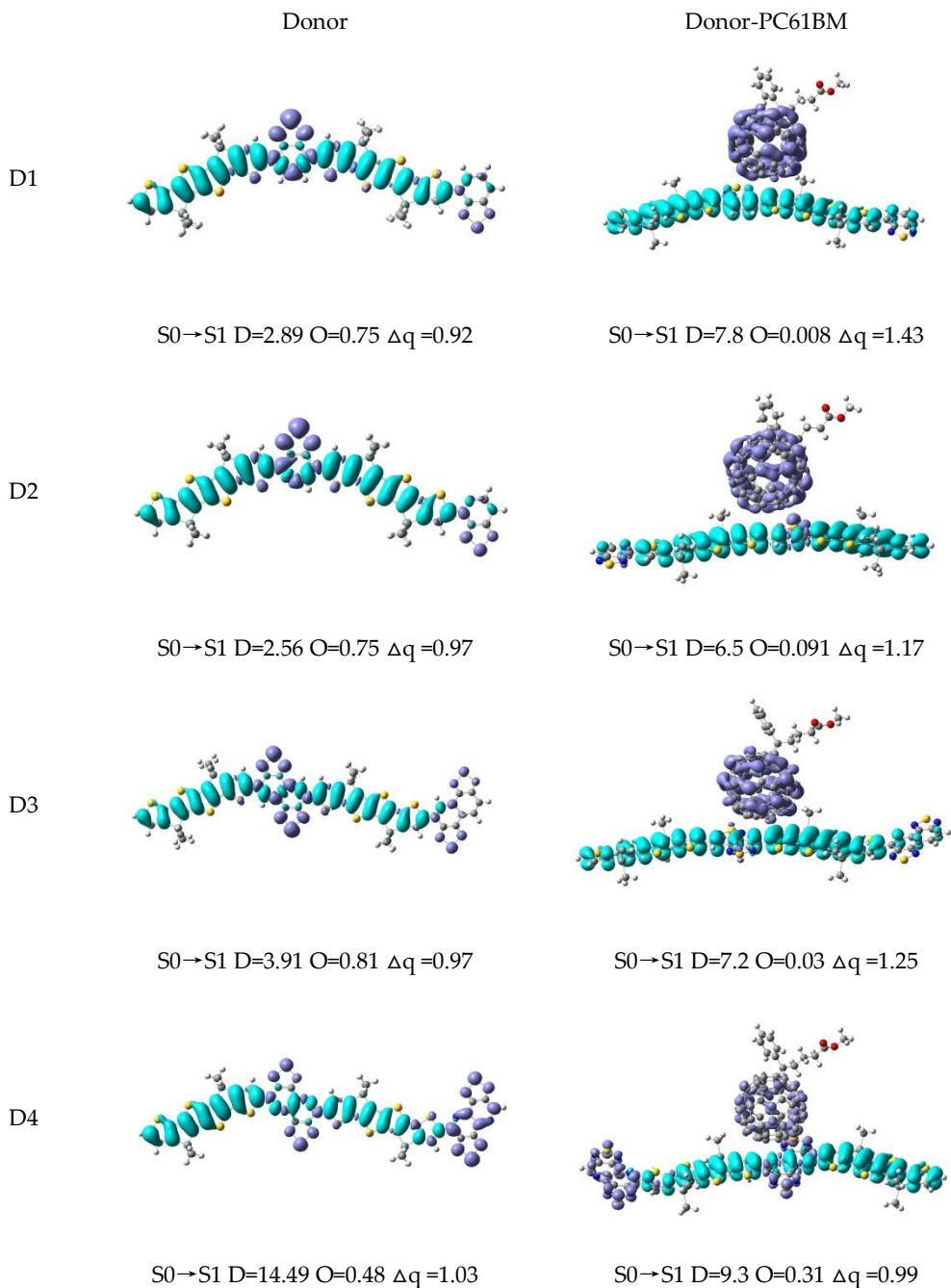


Figure 6: Electron density difference plots of studies dimers

The transfer integral was directly affected by the way of intermolecular stacking. Face to face molecular stacking is a popular method to theoretical simulation molecular stacking at

present for its relative veracity and simplification [40]. In this work, MPW1PBE, MPW1LYP, PW91, M062X, PBE0 and B3PW91 functional under 6-31G(d) basis level were chosen to find the most stable position of two adjacent segments. And scanning plots for the π -stacking distance of two adjacent segments by those functional (supporting information Figure S1) denotes that the lowest energy point could be found under M062X/6-31G(d) level (Figure S3). Hence, this functiona was employed to scan the π -stacking distance of two adjacent segments of the four dimers.

The scanned π -stacking distance (d) of two adjacent segments, reorganization energy (λ_h), The calculated hole coupling strength (V_h), hole transfer rate (K_h) and carrier drift mobility (μ_h) for four dimers were listed in Table 5. The scanned π -stacking distances for D1/D2/D3/D4 are 3.640/3.590/3.600/3.530 Å respectively. The monocycle based D1 and D2, and fused cyclic based D3 and D4 shows the approximate λ_h (0.252/0.259 eV and 0.219/0.217 eV respectively), the value of fused cyclic based dimers are smaller than that of monocycle based counterparts. In addition, values of V_h for D1/D2/D3/D4 is 0.083/0.077/0.079/0.089 eV respectively. As for K_h , the four dimers are in the same order, for instance 2.01, 1.59, 2.68 and 3.49×10^{13} s⁻¹ respectively. And the value of fused cyclic based molecules are larger than that of monocycle based counterparts, besides, the pyridine introduced fused cyclic based polymer proves advantageous. The carrier drift mobility μ_h related to hole transfer rate is 0.517/0.399/0.677/0.846. The result can further prove the positive effect of fused cyclic based molecules and pyridine introduced fused cyclic based polymer. Just for the reason of that fused cyclic and pyridine introduced fused cyclic based structure are conducive to the hole transfer mainly by reduce reducing the reorganization energy.

In general, fused cyclic based polymers have a better hole transfer properties than their counterparts, and pyridine introduced fused cyclic based polymers do positive effects on transfer properties, while pyridine introduced monocycle based polymers have no such significant enhancement.

Table 5. Intermolecular distances (d), reorganization energy (λ_h), the calculated hole coupling (V_h), hole transfer rate (k_h) and hole Mobilities (μ_h) of the studied dimers.

<i>molecules</i>	<i>d/nm</i>	λ_h/eV	V_h/eV	k_h/s^{-1}	$\mu_h/\text{cm}^2 \cdot (\text{V} \cdot \text{S})^{-1}$
D1	3.640	0.252	0.083	2.01×10^{13}	0.517
D2	3.590	0.259	0.077	1.59×10^{13}	0.399
D3	3.600	0.219	0.079	2.68×10^{13}	0.677
D4	3.530	0.217	0.089	3.49×10^{13}	0.846

4. Conclusion

In this work, the electronic and optical properties of four dimers were discussed by

theoretical method with DFT and TD-DFT theory under PBE0/6-31G(d) level, and the influence of the introduction of pyridine and fused cyclic to the polymer properties were also studied. The results show that the planarity of pyridine based and fused cyclic based polymers are better than their corresponding polymer, and lower HOMO energy can achieve to get a higher V_{oc} . Besides, the research on the absorption properties revealed that the pyridine based and fused cyclic based polymer possesses a broader and stronger absorption spectra so can get a large J_{sc} compared with their counterparts. Moreover, the introduction of pyridine on fused cyclic based polymer exhibits enhancement of hole transfer rate mainly due to the reduction of the reorganization energy. Hence we concluded that the introduction of pyridine and fused cyclic, as a donor polymer of organic solar cells, could improve the performance of the devices, and the above results may provide a guideline of structural modification for further investigation on polymer solar cells.

Acknowledgements

We acknowledge generous financial support from Natural Science Foundation of China (21173169, 20803059), ChongqingMunicipal Natural Science Foundation (cstc2013jcyjA90015).

References

- [1] Y. Lin, Y. Li, X. Zhan, Small molecule semiconductors for high-efficiency organic photovoltaics, *Chemical Society Reviews*, 41 (2012) 4245-4272.
- [2] S. Günes, H. Neugebauer, N.S. Sariciftci, Conjugated polymer-based organic solar cells, *Chemical reviews*, 107 (2007) 1324-1338.
- [3] C. Duan, F. Huang, Y. Cao, Recent development of push-pull conjugated polymers for bulk-heterojunction photovoltaics: rational design and fine tailoring of molecular structures, *Journal of Materials Chemistry*, 22 (2012) 10416-10434.
- [4] S. Tang, J. Zhang, Rational design of organic asymmetric donors D1-A-D2 possessing broad absorption regions and suitable frontier molecular orbitals to match typical acceptors toward solar cells, *Journal of Physical Chemistry A*, 115 (2011) 5184-5191.
- [5] Z.G. Zhang, J. Wang, Structures and properties of conjugated Donor-Acceptor copolymers for solar cell applications, *Journal of Materials Chemistry*, 22 (2012) 4178-4187.
- [6] R.G. Parr, W. Yang, *Density-functional theory of atoms and molecules*, Oxford university press, 1989.
- [7] C. Lee, W. Yang, R.G. Parr, Development of the Colle-Salvetti correlation-energy formula into a functional of the electron density, *Physical Review B*, 37 (1988) 785.
- [8] A.D. Becke, Density-functional thermochemistry. III. The role of exact exchange, *The Journal of Chemical Physics*, 98 (1993) 5648-5652.
- [9] Z. Li, S.W. Tsang, X. Du, L. Scoles, G. Robertson, Y. Zhang, F. Toll, Y. Tao, J. Lu, J. Ding, Alternating Copolymers of Cyclopenta [2, 1-b; 3, 4-b'] dithiophene and Thieno [3, 4-c] pyrrole-4, 6-dione for

- High-Performance Polymer Solar Cells, *Advanced Functional Materials*, 21 (2011) 3331-3336.
- [10] A.D. Becke, Density-functional thermochemistry. IV. A new dynamical correlation functional and implications for exact-exchange mixing, *The Journal of chemical physics*, 104 (1996) 1040-1046.
- [11] Y. Li, T. Pullerits, M. Zhao, M. Sun, Theoretical characterization of the PC60BM: PDDTT model for an organic solar cell, *The Journal of Physical Chemistry C*, 115 (2011) 21865-21873.
- [12] L.M. Tolbert, Solitons in a box: the organic chemistry of electrically conducting polyenes, *Accounts of chemical research*, 25 (1992) 561-568.
- [13] A.D. Boese, J.M.L. Martin, N.C. Handy, The role of the basis set: Assessing density functional theory, *Journal of Chemical Physics*, 119 (2003) 3005-3014.
- [14] Y. Zhao, D.G. Truhlar, The M06 suite of density functionals for main group thermochemistry, thermochemical kinetics, noncovalent interactions, excited states, and transition elements: two new functionals and systematic testing of four M06-class functionals and 12 other functionals, *Theoretical Chemistry Accounts*, 120 (2008) 215-241.
- [15] M. Frisch, G. Trucks, H.B. Schlegel, G. Scuseria, M. Robb, J. Cheeseman, G. Scalmani, V. Barone, B. Mennucci, G. Petersson, Gaussian 09, Revision A. 02, Gaussian, Inc., Wallingford, CT, 200 (2009).
- [16] S. Tang, J. Zhang, Rational design of organic asymmetric donors D1-A-D2 possessing broad absorption regions and suitable frontier molecular orbitals to match typical acceptors toward solar cells, *The Journal of Physical Chemistry A*, 115 (2011) 5184-5191.
- [17] M.A. Uddin, T.H. Lee, S. Xu, S.Y. Park, T. Kim, S. Song, T.L. Nguyen, S.-j. Ko, S. Hwang, J.Y. Kim, H.Y. Woo, Interplay of Intramolecular Noncovalent Coulomb Interactions for Semicrystalline Photovoltaic Polymers, *Chemistry of Materials*, 27 (2015) 5997-6007.
- [18] M.C. Scharber, D. Mühlbacher, M. Koppe, P. Denk, C. Waldauf, A.J. Heeger, C.J. Brabec, Design rules for donors in bulk-heterojunction solar cells—Towards 10% energy-conversion efficiency, *Advanced Materials*, 18 (2006) 789-794.
- [19] J. Ku, Y. Lansac, Y.H. Jang, Time-dependent density functional theory study on benzothiadiazole-based low-band-gap fused-ring copolymers for organic solar cell applications, *The Journal of Physical Chemistry C*, 115 (2011) 21508-21516.
- [20] M. Lo, T. Ng, T. Liu, V. Roy, S. Lai, M. Fung, C. Lee, S. Lee, Limits of open circuit voltage in organic photovoltaic devices, *Applied physics letters*, 96 (2010) 113303-113303-113303.
- [21] J. Bijleveld, R. Verstrijden, M. Wienk, R. Janssen, Maximizing the open-circuit voltage of polymer: Fullerene solar cells, *Applied Physics Letters*, 97 (2010) 073304-073304-073303.
- [22] T. Earmme, Y.-J. Hwang, N.M. Murari, S. Subramaniam, S.A. Jenekhe, All-Polymer Solar Cells with 3.3% Efficiency Based on Naphthalene Diimide-Selenophene Copolymer Acceptor, *Journal of the American Chemical Society*, 135 (2013) 14960-14963.
- [23] C. Risko, M.D. McGehee, J.-L. Brédas, A quantum-chemical perspective into low optical-gap polymers for highly-efficient organic solar cells, *Chemical Science*, 2 (2011) 1200-1218.
- [24] R. ShahidáAshraf, J. Andrew, P. ShakyáTuladhar, Synthesis of novel thieno [3, 2-b] thienobis

- (silolothiophene) based low bandgap polymers for organic photovoltaics, *Chemical Communications*, 48 (2012) 7699-7701.
- [25] E. Zhou, J. Cong, K. Tajima, C. Yang, K. Hashimoto, Synthesis and photovoltaic properties of donor-acceptor copolymer based on dithienopyrrole and thienopyrroledione, *Macromolecular Chemistry and Physics*, 212 (2011) 305-310.
- [26] G. Zhang, C.B. Musgrave, Comparison of DFT methods for molecular orbital eigenvalue calculations, *The Journal of Physical Chemistry A*, 111 (2007) 1554-1561.
- [27] Y. Li, Molecular design of photovoltaic materials for polymer solar cells: toward suitable electronic energy levels and broad absorption, *Accounts of chemical research*, 45 (2012) 723-733.
- [28] R. Marcus, Chemical and electrochemical electron-transfer theory, *Annual Review of Physical Chemistry*, 15 (1964) 155-196.
- [29] Y. Shang, Q. Li, L. Meng, D. Wang, Z. Shuai, Computational characterization of organic photovoltaic devices, *Theoretical Chemistry Accounts*, 129 (2011) 291-301.
- [30] I. Volfan, Small polaron model of the electron motion in organic molecular crystals, *physica status solidi (b)*, 59 (1973) 351-360.
- [31] L. Wang, G. Nan, X. Yang, Q. Peng, Q. Li, Z. Shuai, Computational methods for design of organic materials with high charge mobility, *Chemical Society Reviews*, 39 (2010) 423-434.
- [32] C. Wang, F. Wang, X. Yang, Q. Li, Z. Shuai, Theoretical comparative studies of charge mobilities for molecular materials: Pet versus bnpery, *Organic Electronics*, 9 (2008) 635-640.
- [33] G.R. Hutchison, M.A. Ratner, T.J. Marks, Hopping transport in conductive heterocyclic oligomers: reorganization energies and substituent effects, *Journal of the American Chemical Society*, 127 (2005) 2339-2350.
- [34] B.C. Lin, C.P. Cheng, Z.P.M. Lao, Reorganization energies in the transports of holes and electrons in organic amines in organic electroluminescence studied by density functional theory, *The Journal of Physical Chemistry A*, 107 (2003) 5241-5251.
- [35] S. Yin, Y. Yi, Q. Li, G. Yu, Y. Liu, Z. Shuai, Balanced Carrier Transports of Electrons and Holes in Silole-Based Compounds A Theoretical Study, *The Journal of Physical Chemistry A*, 110 (2006) 7138-7143.
- [36] X. Liu, R. He, W. Shen, M. Li, Molecular design of donor-acceptor conjugated copolymers based on C-, Si- and N-bridged dithiophene and thienopyrroledione derivatives units for organic solar cells, *Journal of Power Sources*, 245 (2014) 217-223.
- [37] L. Wang, H. Zhang, Impact of Methylchalcogeno Substitution on the Electronic and Charge Transport Properties of Bis (methylchalcogeno) acenes, *The Journal of Physical Chemistry C*, 115 (2011) 20674-20681.
- [38] Y.-K. Lan, C.-I. Huang, A Theoretical Study of the Charge Transfer Behavior of the Highly Regioregular Poly-3-hexylthiophene in the Ordered State, *The Journal of Physical Chemistry B*, 112 (2008) 14857-14862.

- [39] S.-H. Wen, A. Li, J. Song, W.-Q. Deng, K.-L. Han, W.A. Goddard III, First-principles investigation of anisotropic hole mobilities in organic semiconductors, *The Journal of Physical Chemistry B*, 113 (2009) 8813-8819.
- [40] J.-L. Brédas, D. Beljonne, V. Coropceanu, J. Cornil, Charge-transfer and energy-transfer processes in π -conjugated oligomers and polymers: a molecular picture, *Chemical Reviews*, 104 (2004) 4971-5004.